infrastructures

MDPI

Article

Physics-Based Energy Modeling and Electrification Scenarios for Bus Transit Systems: Evidence from Real-World Data

Sofia Borgosano *, Andrea Di Martino and Michela Longo

Department of Energy, Politecnico di Milano, 20156 Milan, Italy; andrea.dimartino@polimi.it (A.D.M.); michela.longo@polimi.it (M.L.)

* Correspondence: sofia.borgosano@polimi.it

Abstract

The decarbonization of urban public transport requires robust tools to evaluate the operational feasibility and energy implications of bus electrification. This study presents a physics-based modeling framework for estimating the energy consumption of urban bus operations using real-world telemetry data. GPS measurements collected onboard operating buses are used to reconstruct vehicle speed profiles and driving dynamics. The methodology is applied to a representative urban bus route operating in the city centre of Milan, characterized by dense traffic, closely spaced stops, and a high density of signalized intersections. Two operational improvement scenarios are investigated: traffic signal coordination through a "green wave" strategy and the integration of opportunity flash charging (OC) at selected stops. The results show that reducing traffic-related stops improves commercial speed and decreases energy demand, while OC can support battery operation within the constraints of urban service conditions. The proposed framework provides a transferable decision-support methodology for transit agencies planning the electrification of urban bus services and the deployment of supporting infrastructure.

Keywords: electric buses; energy consumption modeling; sustainable mobility; local public transport

1. Introduction

Urban transportation plays a central role in the global transition towards low-carbon mobility. Local Public Transportation (LPT) systems, and especially bus fleets, represent a strategic sector for reducing greenhouse gas emissions and improving air quality in densely populated urban areas [1,2]. In this context, the electrification of urban bus fleets has gained strong momentum under the European Green Deal and related national decarbonization policies [3,4]. Cities are progressively deploying Battery Electric Buses (BEBs) as part of large-scale fleet renewal programs aimed at reducing urban emissions and improving local air quality. Relevant applications in metropolitan areas all over the world highlight the increasing relevance of BEBs in compact urban environments characterized by high service frequency, congestion, and complex traffic management systems [5–8].

However, the transition introduces several technical and operational challenges. Compared to conventional Internal Combustion Engine (ICE) vehicles, BEBs are constrained by inherent limitations of current battery technologies. In particular, the onboard energy storage capacity is restricted, which reduces the achievable driving range under real operating conditions. These conditions include stop-and-go traffic, auxiliary energy use such as heating and air conditioning, and variations in passenger load. In addition, the usable

Check for updates

Academic Editor: António Couto

Received: 20 March 2026
Revised: 20 April 2026
Accepted: 27 April 2026
Published: 29 April 2026

Copyright: © 2026 by the authors. Licensee MDPI, Basel, Switzerland. This article is an open access article distributed under the terms and conditions of the Creative Commons Attribution (CC BY) license.

capacity is further reduced by operational safety margins and gradual performance degradation over time, which can progressively limit vehicle autonomy throughout the battery lifetime [9–12]. These constraints have direct implications for service planning, requiring careful alignment between route length and span, and charging opportunities [13].

Reliable energy models are essential to support decisions on battery sizing, charging infrastructure deployment, and service planning. Energy consumption in urban bus operations is influenced by multiple factors, including vehicle mass, passenger load, driving behavior, road gradient and traffic conditions [14,15]. Additionally, frequent stop-and-go events caused by closely spaced bus stops, signalized intersections, and congestion introduce significant variability in driving cycles, which strongly affects energy demand. Therefore, capturing the interaction between vehicle dynamics and real-world operating conditions is essential for accurate energy assessment.

Existing approaches for estimating the energy consumption of electric buses can generally be classified into data-driven and physics-based methods. Data-driven approaches rely on large datasets and machine learning techniques to predict energy demand based on historical data [16–21]. While these methods can achieve high predictive accuracy, they often require extensive datasets and may lack physical interpretability when applied to different operating contexts. On the other hand, physics-based models provide a more transparent representation of vehicle behavior, but are often based on simplified or standardized driving cycles that may not adequately reflect real-world conditions [22,23]. Recent research has highlighted the importance of using real-world operational data to improve the reliability of energy consumption assessments for electric buses [17,24]. GPS-based telemetry systems allow the collection of detailed information about vehicle position, speed, and travel time, enabling the reconstruction of realistic driving cycles under actual traffic conditions. The integration of such real-world data into vehicle energy models can significantly improve the accuracy of energy consumption estimates and provide a more reliable basis for evaluating electrification strategies. Despite the growing body of literature, several research gaps remain. First, many studies rely on simplified driving cycles or lack direct integration of real-world telemetry data into physics-based models. Second, existing approaches often analyze vehicle energy consumption independently from traffic conditions and operational constraints. Third, limited attention has been given to the combined evaluation of traffic management strategies and charging infrastructure within a unified modeling framework.

In addition to vehicle energy consumption, traffic management strategies can also play an important role in improving the operational efficiency of urban bus services. Frequent stops at signalized intersections increase travel time and energy consumption due to repeated acceleration phases. Traffic signal coordination strategies, such as transit signal priority or green wave (GW) systems, aim to reduce unnecessary stops and improve traffic flow along urban corridors [25,26]. These strategies can generate system-wide effects, influencing not only the performance of individual vehicles but also overall traffic dynamics, including interactions with private vehicles and other public transportation services. Previous studies have shown that coordinated signal control can improve traffic efficiency, reduce delays, and contribute to lower energy consumption and emissions at the network scale [27,28].

Another key aspect in bus electrification is the integration of charging infrastructure. Opportunity charging (OC) systems, such as flash charging at bus stops, allow vehicles to recharge during short dwell times, enabling continuous operation with reduced battery capacity [11,29]. The effectiveness of such solutions strongly depends on route characteristics, dwell times, and operational patterns, thus highlighting the need for modeling frameworks that jointly consider vehicle dynamics, traffic conditions, and infrastructure constraints [30–32].

In this context, this study proposes a physics-based modeling framework for the evaluation of the energy consumption and operational performance of urban bus systems using real-world GPS telemetry data. The approach reconstructs realistic driving cycles directly from measured speed profiles and integrates them into a longitudinal vehicle dynamics model, allowing detailed estimations of traction and auxiliary power consumption, and regenerative braking under actual operating conditions. The proposed methodology addresses key limitations in the literature by combining real-world data with a physically grounded modeling approach, while explicitly accounting for traffic-related disturbances and operational constraints. In addition, the framework enables the integrated assessment of traffic signal coordination and opportunity charging strategies within a unified simulation environment. The methodology is applied to a representative urban bus route in Milan, providing insights into the interaction between traffic conditions, service performance, and energy demand. Although the analysis is conducted at the route level, the eligible strategies, particularly traffic signal coordination, are discussed in the context of broader network-level implementations, where system-wide effects may influence their overall effectiveness. The main contributions of this work can be summarized as follows:

- The development of a physics-based energy consumption model for urban buses based on real-world GPS telemetry data;
- The reconstruction of realistic driving cycles capturing the variability of traffic conditions and operational constraints;
- The integrated evaluation of traffic signal coordination and opportunity charging strategies within a unified framework;
- Application to a real-world case study, providing quantitative insight into the relationship between traffic conditions, operational efficiency, and energy consumption.

The remainder of the paper is organized as follows. Section 2 presents the proposed methodology while Section 3 describes the urban case study in Milan and analyzes the operational characteristics of the selected bus route using real-world data. Section 4 presents the simulation results and evaluates the impact of traffic signal coordination and opportunity flash-charging strategies.

2. Methodology

The physics-based energy consumption model was adopted and implemented to analyze the actual bus operations on a selected line. This model can be easily replicated for other vehicle types and line routes, with sensibly different topography profiles. The modeling strategy adopted is strongly dependent on the availability of data to be either disclosed or acquired during public service. Operational data were collected through on-board telemetry using a smartphone-based GPS logging application. The system recorded position and speed at a sampling frequency of 20 Hz. These measurements were used to reconstruct the vehicle speed profile and derive acceleration and traveled distance. The overall simulation workflow adopted in this study is illustrated in Figure 1. The framework integrates telemetry data processing throughout:

- A longitudinal vehicle dynamics model;
- A stop analysis, with evaluation of improvements due to the green wave strategy;
- Opportunity flash-charging (OC) simulation.

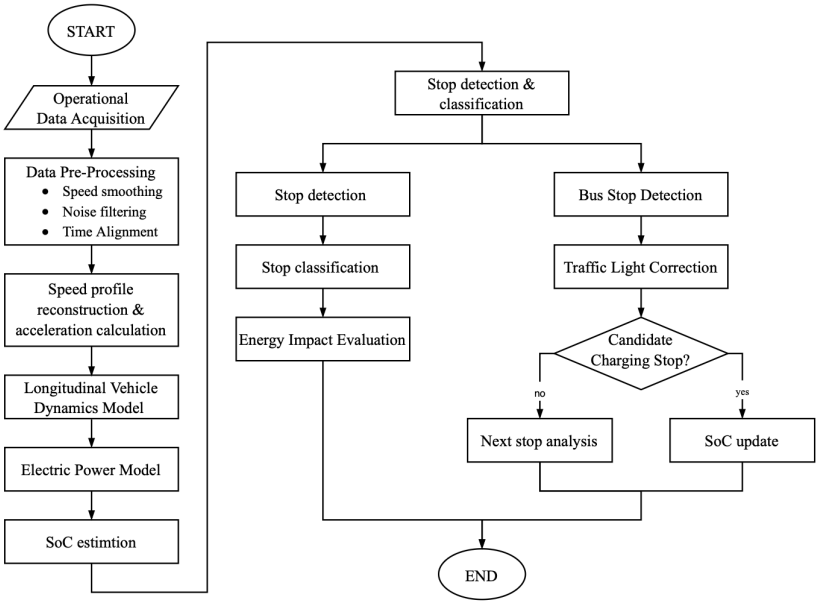

Figure 1. Schematic representation of the simulation framework adopted in this study.

2.1. Longitudinal Vehicle Dynamics Model

The longitudinal vehicle dynamics model is exploited to estimate traction forces, the electric power demand, and the cumulative energy consumption of the vehicle based on the measured speed data. The model is grounded on the balance of longitudinal forces and includes rolling resistance, aerodynamic drag, inertial effects, and regenerative braking. To reduce noise interference in the measured signal, the velocity is smoothed using a centered moving average over a window defined by (1), where N is the moving-average window length in samples, Gap_{second} denotes the smoothing interval in seconds, and f_s is the sampling frequency in hertz.

$$N = \frac{Gap_{second}}{f_s} \tag{1}$$

Acceleration is computed from the smoothed velocity signal using a finite difference approach reported in (2), where $\Delta(t)$ corresponds to the aggregated time interval of the smoothing window.

$$a(t) = \frac{v(t + \Delta t) - v(t)}{\Delta t} \tag{2}$$

The Total Force F_T required at the wheels can be expressed as the sum of inertial effects F_i, rolling resistance F_r, aerodynamic drag F_a, and gravitational forces (F_g) due to sloped road profiles as reported in (3).

$$F_{tot} = F_i + F_r + F_a + F_g \tag{3}$$

The electric power demand includes the auxiliary power consumption and the traction power. During this phase or when the vehicle is being accelerated or traveling at constant speeds, drivetrain losses η_t must be considered. Conversely, during the braking phase, the regenerative braking efficiency η_b, and regenerative braking fraction β_{reg} must be considered. The two formulations are therefore reported in (4).

$$P_{el}(t) = \begin{cases} P_{aux} + \dfrac{P_{tr}(t)}{\eta_t}, & P_{tr}(t) > 0 \\ P_{aux} + P_{tr}(t)\eta_b\beta_{reg}, & P_{tr}(t) \leq 0 \end{cases} \quad (4)$$

The energy consumption during the whole driving cycle is calculated by integrating the power demand over time, as reported in (5).

$$E_{el}(t) = \sum \frac{P_{el}(t) \cdot \Delta(t)}{3600} \quad (5)$$

This modeling framework enables the estimation of the vehicle energy demand based on the speed profile of the route and the physical characteristics of the vehicle. The approach can be applied to different vehicle technologies by adapting the drivetrain efficiency and energy conversion parameters.

2.2. Stop Analysis and Green Wave Introduction

With the vehicle physical model defined, the simulation framework is extended by integrating an energy management module that combines vehicle energy consumption with the energy supplied by OC infrastructure. The aim of this module is to simulate the dynamic interaction between vehicle operation and the effectiveness of high-power flash-charging stations placed along the route. To evaluate the operational efficiency of the route, a stop detection algorithm was implemented using the vehicle speed profile derived from GPS measurements. A vehicle is considered stationary when its instantaneous speed falls below a predefined threshold of 1 km/h. Due to sensor inaccuracies, recorded speed values rarely reach exactly zero even when the vehicle is stationary. This threshold allows for a more robust identification of stop events while avoiding misclassifications of very low-speed motion. Consecutive samples satisfying the stop condition are grouped into stop blocks. A stop block therefore represents a continuous period during which the vehicle remains stationary. The duration of each stop block is computed using (6), where j identifies the j-th stop block and Δt_i are the time increments belonging to that block.

$$T_{block,j} = \sum_{i \in j} \Delta t_i \quad (6)$$

The total stopped time along the route is obtained by summing the duration of all stop blocks as in (7).

$$T_{stop} = \sum_{j=1}^{N} T_{block,j} \quad (7)$$

To be able to distinguish between different causes of vehicle stops, each block is classified according to its time duration. Moreover, several threshold values for stop times are introduced to classify the stop type. Short stops are associated with passenger boarding and alighting at bus stops, whereas longer stops are assumed to be related to traffic lights or congestion. The classification rule is defined as in (8), where the threshold (T_{th}) is set to 30 s, selected based on typical dwell times observed in urban bus operations.

$$\begin{cases} T_{block} < T_{th} & \rightarrow \text{Passenger stop} \\ T_{block} \geq T_{th} & \rightarrow \text{Traffic delay} \end{cases} \quad (8)$$

Based on this classification, the total travel time can be decomposed as the sum of time spent in motion (T_{mov}), the passenger service time (T_{stop}) and the time lost due to traffic

signals or congestion (T_{traf}) as reported in (9). This classification enables the identification of operational inefficiencies and provides a quantitative basis for evaluating signal priority strategies and OC opportunities.

$$T_{tot} = T_{mov} + T_{stop} + T_{traff} \tag{9}$$

To reduce stopping times at signalized intersections and to assess the potential benefits of traffic signal coordination, a GW scenario was introduced. The approach assumes that an improved level of coordination enables the vehicle to avoid a portion of the waiting time. Rather than explicitly modeling traffic signal timing and vehicle–infrastructure interactions, a simplified proportional formulation is adopted to approximate this effect. The time savings are therefore expressed as a fraction of the original stop duration, as reported in (10), where the parameter α represents the share of time that can be effectively avoided. It depends on the degree of synchronization between traffic signals and bus operations, and may vary depending on infrastructure and traffic conditions.

$$T_{saved} = \alpha \cdot T_{block} \tag{10}$$

This formulation provides a first-order estimation of the potential impact of GW strategies, while maintaining a low level of model complexity. The total travel time under the GW scenario is therefore calculated according to (11).

$$T_{new} = T_{tot} - \sum T_{saved} \tag{11}$$

The energetic impact of avoiding a stop, reported in (12), is computed through a simplified energy balance. Different contributions are considered as follows:

1. Auxiliary Energy Saving (E_{aux}): Auxiliary systems such as air conditioning and lighting consume less energy.
2. Restart Energy Saving ($E_{restart}$): Avoiding a full stop eliminates the energy required to accelerate the vehicle from a standstill position. This energy is estimated from the measured traction power in the seconds following each stop.
3. Lost Regenerative Energy (E_{reg}): If the vehicle does not stop, the regenerative braking energy that would have been recovered during deceleration is partially lost.
4. Maintain Energy Required (E_{main}): This is the energy required to maintain motion through the intersection with an average speed of 20 km/h.

$$E_{net} = E_{tot} - \sum E_{save} \tag{12}$$

$$E_{save} = E_{aux} + E_{restart} - (E_{reg} + E_{main})$$

2.3. Flash Charging

To identify potential OC locations, an analysis of dwell times for bus stops was conducted using GPS trajectory data combined with vehicle speed measurements. For each stop location, the vehicle position was compared with the geographic coordinates of the stop using a circular spatial buffer. A stop event was detected when the conditions in (13) and (14) were simultaneously satisfied, where

- d_i is the distance between the vehicle and the target stop;
- r is the spatial detection radius equal to 30 m;
- v_i is the instantaneous vehicle speed;
- v_{tr} is the stop threshold velocity equal to 0.5 km/h.

$$d_i < r \tag{13}$$

$$v_i < v_{tr} \tag{14}$$

The total dwell time at stop j ($T_{stop,j}$) is therefore computed using (15), where S_j represents the set of samples meeting the stop conditions.

$$T_{stop,j} = \sum_{i \in S_j} \Delta t_i \tag{15}$$

In urban environments, part of the measured dwell time may be caused by traffic light delays rather than passenger boarding. To avoid overestimating the available charging time, a correction was applied to stops located close to traffic lights. If the dwell time exceeded a predefined threshold (40 s), a red-light penalty of 20 s was subtracted (T_{red}). This correction prevents overestimation of the effective charging time and is consistent with typical urban signal cycle delays. If no traffic signal is associated with the stop, the dwell time is assumed to be caused primarily by passenger boarding. The corrected dwell time is therefore reported in (16).

$$T_{corr,j} = \begin{cases} T_{stop,j} - T_{red} & \text{traffic signal} \\ T_{stop,j} & \text{otherwise} \end{cases} \tag{16}$$

A stop was classified as a charging candidate when $T_{corr,j}$ was higher than 15 s. The minimum dwell time threshold ensures that sufficient time is available for pantograph connection and effective energy transfer. Charging is activated when the vehicle reaches a charging stop and remains within the detection radius. After an automatic pantograph connection time ($T_{connect}$) the charging process starts. The charging power (P_{charge}) was assumed constant and the energy transferred during a charging event was calculated using (17), where T_{charge} is the available dwell time at the stop.

$$E_{charge} = P_{charge} \cdot \frac{T_{charge}}{3600} \tag{17}$$

The battery SoC is therefore updated according to (18), where E_{batt} is the battery capacity of the vehicle.

$$SoC_{t+1} = SOC_t - \frac{P_{net} \cdot \Delta t}{E_{batt}} \tag{18}$$

3. Case Study

The selected case study focuses on a typical urban bus route located in the center of Milan. Milan represents a relevant case study for urban mobility analysis due to the scale and intensity of its public transport system. A high passenger demand, combined with dense urban traffic conditions and a large number of signalized intersections, makes Milan an appropriate case study for evaluating the interactions between traffic management strategies, operational performances, and energy consumption in electric bus systems.

To ensure a robust analysis, a total of eight trips were considered, including four inbound and four outbound journeys. The selected case study corresponds to bus line 62, which covers approximately 7.8 km and connects the city center with surrounding districts such as Porta Romana and Leoncavallo. The route operates in a densely populated urban environment, characterized by frequent intersections and complex traffic conditions. Figure 2 illustrates the layout of the route within the urban road network.

The operational context is characterized by:

- The absence of dedicated bus lanes, resulting in significant interference with private traffic.
- A high density of traffic lights and intersections: 7.75 traffic-light/km corresponding to an average spacing of ∼129 m.
- Closely spaced bus stops, with an average inter-stop distance of 320 m.

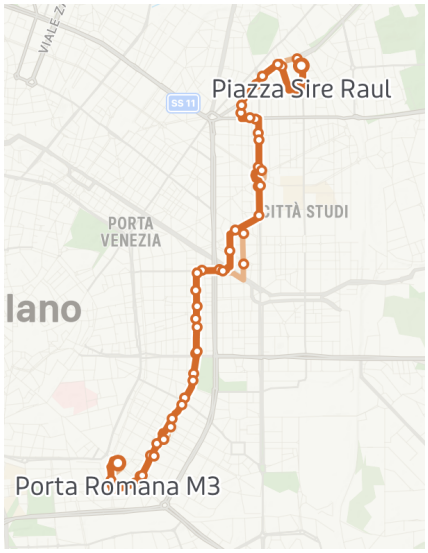

Figure 2. Analyzed bus route (Line 62) within the Milan urban road network.

These conditions result in frequent stop-and-go operations and reduced service regularity. To obtain representative passenger demand patterns, two average load profiles were generated, one for each travel direction. The number of passengers boarding at each stop was calculated as the mean value across all trips and rounded to the nearest unit. The resulting profiles are shown in Figure 3 for the inbound and outbound directions. The demand distribution appears relatively uniform along the route, with no significant peaks. The average onboard occupancy is approximately 18 passengers.

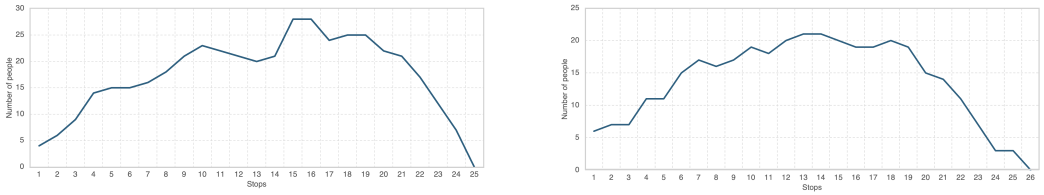

(**a**) (**b**)

Figure 3. Average passenger load profiles along the route for (**a**) inbound and (**b**) outbound directions.

The model was parameterized based on the technical specifications of a Solaris Urbino 12 electric bus, in order to evaluate the proposed methodology on a representative heavy-duty vehicle. The parameters used in the vehicle dynamics and powertrain model are reported in Table 1. The adopted values are derived from manufacturer specifications or selected according to representative ranges reported in the literature for similar urban electric bus applications, in order to ensure a realistic and consistent operational representation [33,34]. In particular, the traction efficiency ($\eta_t = 0.70$) and braking efficiency ($\eta_b = 0.85$) reflect typical drivetrain and energy conversion losses under urban driving conditions. The auxiliary power demand ($P_{aux} = 12$ kW) accounts for the continuous onboard energy consumption associated with systems such as HVAC, lighting, and passenger-related services during operation. The regeneration factor ($\beta_{reg} = 0.70$)

represents the portion of braking energy that can be effectively recovered, considering practical limitations in the energy regeneration process and battery charging constraints.

The combination of low commercial speed, frequent stop occurrences, and moderate but continuous passenger demand makes this urban route a representative case for assessing operational inefficiencies and evaluating the potential benefits of optimized traffic management and electrification strategies.

Table 1. Key parameters of the Solaris Urbino 12 electric bus used in the simulation model.

Parameter	Symbol	Value	Unit
Tare mass	m_{empty}	13,500	kg
Drag coefficient	C_x	0.60	–
Frontal area	A_f	8.415	m^2
Rolling resistance coefficient	f_v	0.01	–
Maximum traction power	P_{max}	250	kW
Maximum traction force	F_{max}	40,000	N
Auxiliary power demand	P_{aux}	12	kW
Traction efficiency	η_t	0.70	–
Braking efficiency	η_b	0.85	–
Regeneration factor	β_{reg}	0.70	–
Comfort acceleration limit	a_{max}	1.5	m/s^2

4. Results and Discussion

This section presents the results obtained from the application of the proposed energy modeling framework to the selected urban bus route. The analysis aims to evaluate the operational and energetic performance of the system under real-world conditions.

4.1. Energy Analysis

The energy consumption associated with the analyzed trips is evaluated to quantify the sensitivity of the system to realistic driving variability under urban operating conditions. As shown in Figure 4, total energy demand exhibits a clear dispersion across trips, despite all simulations being conducted over the same route. This indicates that route topology alone is not sufficient to determine energy requirements; instead, operational dynamics play a dominant role. From a quantitative perspective, the simulated energy consumption ranges between 14.44 kWh and 17.77 kWh, with a mean value of 16.60 kWh and a standard deviation of approximately 1.07 kWh (coefficient of variation ≈ 6.5%). This indicates a moderate but non-negligible variability in energy demand under consistent route conditions.

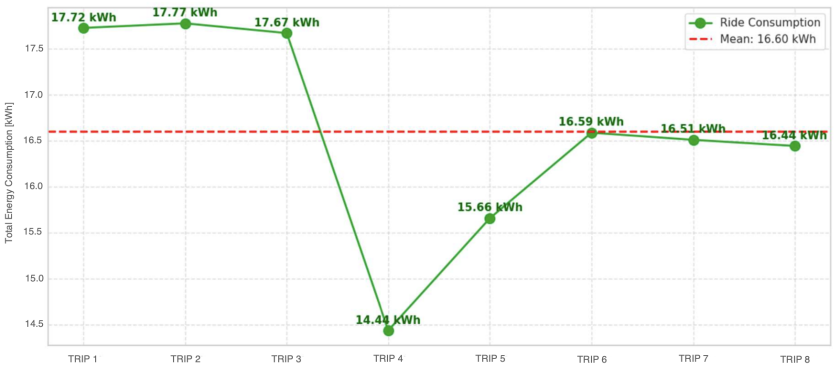

Figure 4. Total energy consumption per trip for the analyzed bus route under real-world operating conditions.

From a practical perspective, this spread corresponds to a difference of more than 3 kWh between minimum and maximum consumption. This variability is mainly driven by changes in operational conditions. These include traffic intensity, stop frequency and duration, and dynamic driving profiles characterized by frequent acceleration and deceleration phases. Since the proposed model is based on real-world GPS-derived speed data, even small fluctuations in traffic conditions result in measurable differences in energy demand. These findings indicate that energy consumption forecasting for BEBs cannot rely on deterministic assumptions only, but must instead account for stochastic variability in traffic conditions. Incorporating this variability is essential for the design of reliable energy management strategies, as neglecting it may lead to underestimation of energy requirements and reduced operational robustness, particularly in dense urban contexts.

Figure 5 extends the analysis by comparing the environmental performance of the propulsion technologies considered in this study. The results show a pronounced reduction in CO_2 emissions when switching from conventional diesel buses to electric buses across all analyzed trips. This improvement is structurally driven by the higher energy conversion efficiency of the electric drivetrain and the elimination of direct tailpipe emissions during operation. While the analysis is limited to operational-phase emissions, the magnitude of the reduction remains substantial even under varying traffic conditions, indicating that the environmental benefit is robust with respect to route-specific variability.

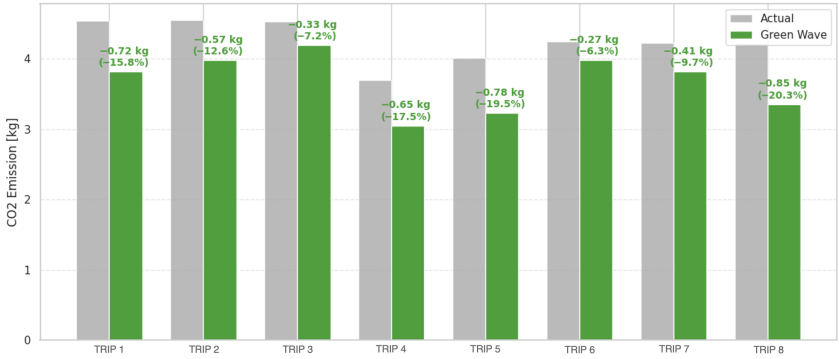

Figure 5. Comparison of CO_2 emissions per trip for different propulsion technologies.

4.2. Impact of GW Strategy

The total travel time can be decomposed into three main components: vehicle motion time, passenger service time at stops, and time lost due to traffic conditions. This analysis shows that a significant fraction of the total travel time is associated with traffic-related delays rather than passenger operations. As shown in Figure 6, traffic-related delays account for a significant share of the total travel time, in most cases comparable to or exceeding passenger service time. This result indicates that operational inefficiencies are primarily driven by external traffic conditions rather than passenger demand, suggesting that traffic management strategies may have a substantial impact on service performance.

The average commercial speed recorded in the analyzed case is approximately 9.78 km/h, which is considerably lower than the typical target of 15 km/h for urban bus services. This gap indicates that the route operates under highly constrained traffic conditions, where frequent stops at traffic signals and interactions with private vehicles significantly reduce operational efficiency. This acts as a proper "worst-case" scenario. Additionally, as shown in Figure 7, the gap between commercial speed and moving speed is consistently large across all trips. This difference quantifies the impact of stopping events and traffic interruptions, confirming that a significant portion of the service time is not spent in effective motion.

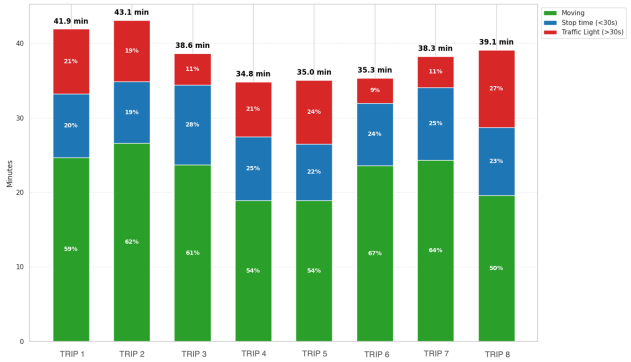

Figure 6. Breakdown of total travel time into vehicle motion time, passenger service time, and traffic-related delays for each trip.

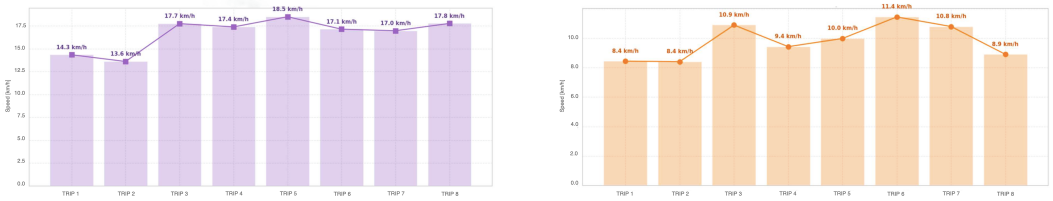

(**a**) (**b**)

Figure 7. Average (**a**) commercial speed and (**b**) moving speed across all analyzed trips.

As a consequence, the concept of the GW strategy was introduced. The impact of the green wave strategy is illustrated in Figure 8. Here a consistent reduction in both travel time and energy consumption across all analyzed trips is depicted. This confirms that minimizing traffic-induced stops not only improves operational efficiency but also reduces energy demand by limiting acceleration phases, which are among the most energy-intensive driving conditions. Additionally, an increase in commercial speed is observed across all analyzed trips, with peak improvements reaching up to 22%. This result further highlights the effectiveness of traffic signal coordination in enhancing service performance, particularly in dense urban environments characterized by frequent stop-and-go conditions.

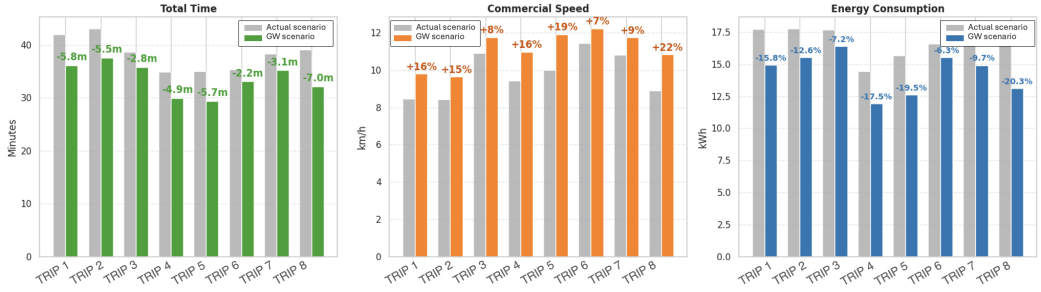

Figure 8. Impact of the green wave strategy on total travel time, commercial speed and energy consumption.

The results obtained should be interpreted in light of the simplifying assumptions adopted in the modeling approach. In particular, the use of a constant proportional factor α to estimate the reduction in traffic-related stop times represents a first-order approximation of traffic signal coordination effects. In real-world conditions, the effectiveness of GW strategies depends on several factors, including traffic demand, signal control logic, intersection spacing, and the level of priority assigned to public transport. As a result, the proportional reduction adopted in this study may overestimate the achievable benefits under non-ideal or highly congested conditions.

4.3. Flash-Charging Simulation

In order to identify the most suitable bus stops for the deployment of flash-charging infrastructure, a detailed stop time analysis was conducted. The results, reported in Figure 9, reveal a strong heterogeneity in dwell times across the investigated stops and scenarios. In particular, the analysis highlights that only a subset of stops systematically provide sufficiently long and stable dwell times, mainly due to signalized intersections and traffic light-induced delays. These locations therefore emerge as the most promising candidates for the installation of charging equipment, as they offer recurrent temporal windows that can be exploited without altering the scheduled service.

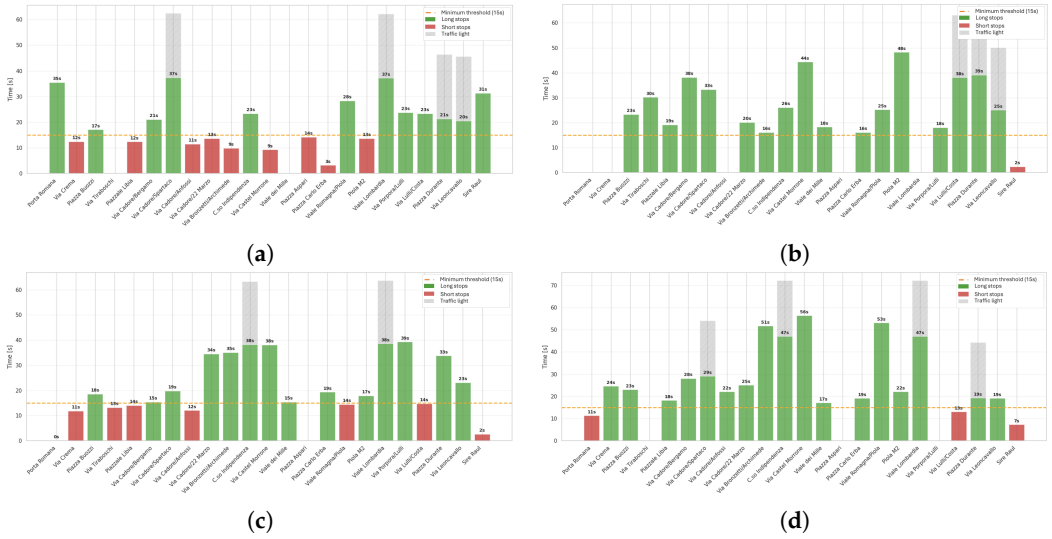

Figure 9. Stop duration of (**a**) Trip 1, (**b**) Trip 3, (**c**) Trip 3 and (**d**) Trip 4.

Building on these findings, Figure 10 shows the resulting energy consumption profiles when flash charging is deployed at the selected stops. Compared to the baseline operation, the introduction of opportunity charging leads to intermittent energy replenishment events during service. This produces a visible smoothing of the SoC trajectory along the route, avoiding deep discharge conditions that are observed in the non-charging case. From an operational perspective, this behavior confirms that flash charging can enhance system resilience by mitigating SoC depletion risks without requiring additional depot charging cycles.

Figure 10 illustrates the simulated energy consumption profile when flash charging is introduced at selected bus stops along the route.

Simulation results show that several stops provide enough dwell time to enable meaningful energy transfer without affecting the operational schedule. As a result, the battery SoC can be partially restored during normal service operations. This strategy offers several operational advantages. In particular, it allows for the reduction in onboard battery capacity installed and extends the operational range of the vehicle without requiring depot charging sessions. A more detailed view of the energy dynamics is provided in Figure 11, which compares the aggregated energy consumption profiles between baseline and flash-charging scenarios. The results indicate a more stable SoC evolution and a reduction in the amplitude of energy deficit peaks, effectively increasing operational robustness and scheduling flexibility.

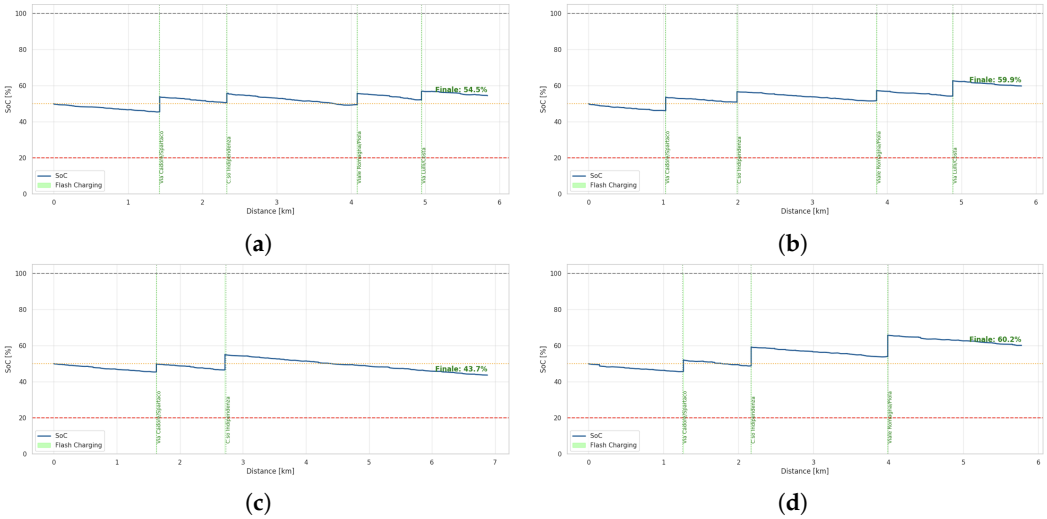

Figure 10. SoC profiles with flash charging for (**a**) Trip 1, (**b**) Trip 2, (**c**) Trip 3 and (**d**) Trip 4.

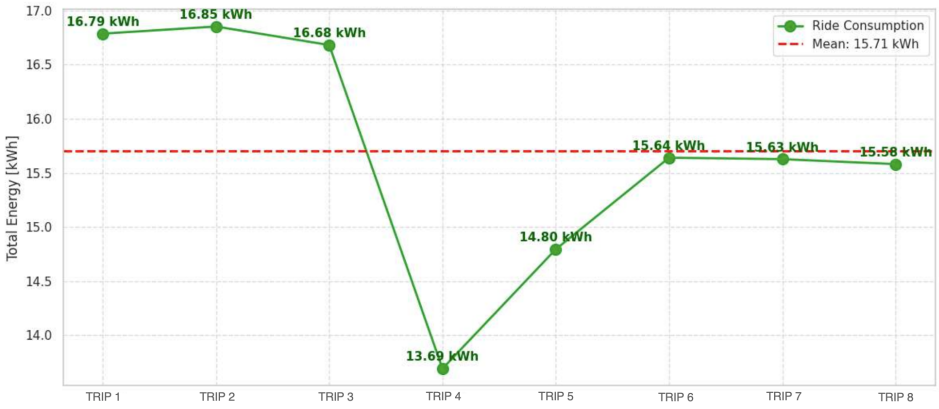

Figure 11. Total energy consumption per trip for the analyzed bus route with flash charging.

These observations are further quantified in Table 2, which compares baseline and charging scenarios across all trips.

Table 2. Comparison of total energy consumption per trip between baseline and flash-charging scenarios.

	Energy Base [kWh]	Energy Charging [kWh]	Δ Energy [kWh]	Δ Energy [%]
Trip 1	17.72	16.79	0.93	−5.24
Trip 2	17.77	16.85	0.92	−5.12
Trip 3	17.67	16.68	0.99	−5.60
Trip 4	14.44	13.69	0.75	−5.19
Trip 5	15.66	14.80	0.86	−5.49
Trip 6	16.59	15.64	0.95	−5.72
Trip 7	16.51	15.63	0.88	−5.33
Trip 8	16.44	15.58	0.86	−5.23
Average	16.60	15.71	0.89	−5.37

5. Conclusions

This study presented a physics-based modeling framework for the evaluation of the energy consumption and operational performance of urban bus systems using real-world GPS telemetry data. The proposed approach enables the reconstruction of realistic driving

cycles and the estimation of vehicle energy demand by combining measured speed profiles with a longitudinal vehicle dynamics model.

The application to a real urban bus route in Milan highlights the strong impact of traffic conditions on both energy consumption and service efficiency. The analysis of stop events showed that traffic-related delays account for approximately 17.9% of the total travel time, leading to frequent stop-and-go operations and increased energy demand. The results demonstrated that traffic signal coordination, such as the implementation of a green wave strategy, can significantly improve operational performance. In particular, the reduction in traffic-related stops led to an increase in commercial speed of approximately +14.0% and an average reduction in total energy consumption of about 13.6%, mainly due to fewer acceleration phases and lower auxiliary energy use during idling. In parallel, the analysis of dwell times confirmed the potential feasibility of opportunity flash-charging solutions in urban environments, showing that selected stops can provide sufficient time for partial energy replenishment without affecting service operations. Overall, the study confirms that the integration of vehicle electrification with traffic management and charging strategies can significantly enhance the efficiency and sustainability of urban bus systems, with potential combined energy savings averaging 5.37% under optimized conditions.

From a transferability perspective, the proposed framework is designed to be general and data-driven, as it relies on GPS-based speed profiles and a physics-based energy model rather than location-specific calibration. However, the quantitative results are inherently dependent on local characteristics such as traffic congestion patterns, signal timing schemes, stop spacing, and passenger demand profiles. Therefore, while the methodological framework can be directly applied to other urban contexts, the magnitude of the observed improvements should be interpreted with respect to the specific operational conditions of the Milan case study. Applying the model to different cities would allow capturing a broader range of urban morphologies and traffic control strategies, further supporting comparative analyses and robust policy evaluation.

Author Contributions: Conceptualization, S.B. and A.D.M.; methodology, S.B.; software, S.B.; validation, S.B., A.D.M. and M.L.; formal analysis, M.L.; investigation, S.B.; resources, M.L.; data curation, S.B.; writing-original draft preparation, S.B.; writing—review and editing, A.D.M.; visualization, A.D.M.; supervision, M.L.; project administration, M.L.; funding acquisition, M.L. All authors have read and agreed to the published version of the manuscript.

Funding: This research received no external funding

Data Availability Statement: Data is unavailable due to privacy restriction

Conflicts of Interest: The authors declare no conflicts of interest.

References

1. Jaworski, A.; Mądziel, M.; Kuszewski, H. Sustainable public transport strategies—Decomposition of the bus fleet and its influence on the decrease in greenhouse gas emissions. *Energies* **2022**, *15*, 2238. [CrossRef]
2. Sacchi, R.; Bauer, C.; Cox, B.; Mutel, C. When, where and how can the electrification of passenger cars reduce greenhouse gas emissions? *Renew. Sustain. Energy Rev.* **2022**, *162*, 112475. [CrossRef]
3. Rimpas, D.; Barkas, D.E.; Orfanos, V.A.; Christakis, I. Decarbonizing the transportation sector: A review on the role of electric vehicles towards the European Green Deal for the new emission standards. *Air* **2025**, *3*, 10. [CrossRef]
4. Soares, F.; Silva, M.; Azevedo, I. Urban decarbonization policies and strategies: A sectoral review. *Renew. Sustain. Energy Rev.* **2025**, *215*, 115617. [CrossRef]
5. Chavez-Baeza, C.; Sheinbaum-Pardo, C. Sustainable passenger road transport scenarios to reduce fuel consumption, air pollutants and GHG (greenhouse gas) emissions in the Mexico City Metropolitan Area. *Energy* **2014**, *66*, 624–634. [CrossRef]
6. Kruchina, V. The possibility of electrification in public transport bus services. *Acta Tech. Jaurinensis* **2023**, *16*, 158–166. [CrossRef]
7. Ginting, M.G.; Reguyal, F.; Cecilia, V.M.; Wang, K.; Sarmah, A.K. Electrification of public buses in Jakarta, Indonesia: A life cycle study. *Sci. Total Environ.* **2024**, *914*, 169875. [CrossRef]

8. Martinez, S.S.; Samaras, C. Electrification of transit buses in the United States reduces greenhouse gas emissions. *Environ. Sci. Technol.* **2024**, *58*, 4137–4144. [CrossRef]
9. Li, J.-Q. Battery-electric transit bus developments and operations: A review. *Int. J. Sustain. Transp.* **2016**, *10*, 157–169. [CrossRef]
10. Pelletier, S.; Jabali, O.; Laporte, G.; Veneroni, M. Battery degradation and behaviour for electric vehicles: Review and numerical analyses of several models. *Transp. Res. Part B Methodol.* **2017**, *103*, 158–187. [CrossRef]
11. Gao, Z.; Lin, Z.; LaClair, T.J.; Liu, C.; Li, J.M.; Birky, A.K.; Ward, J. Battery capacity and recharging needs for electric buses in city transit service. *Energy* **2017**, *122*, 588–600. [CrossRef]
12. Zhou, B.; Wu, Y.; Zhou, B.; Wang, R.; Ke, W.; Zhang, S.; Hao, J. Real-world performance of battery electric buses and their life-cycle benefits with respect to energy consumption and carbon dioxide emissions. *Energy* **2016**, *96*, 603–613. [CrossRef]
13. Rodrigues, A.L.; Seixas, S.R. Battery-electric buses and their implementation barriers: Analysis and prospects for sustainability. *Sustain. Energy Technol. Assess.* **2022**, *51*, 101896. [CrossRef]
14. Lajunen, A. Energy consumption and cost-benefit analysis of hybrid and electric city buses. *Transp. Res. Part C Emerg. Technol.* **2014**, *38*, 1–15. [CrossRef]
15. Basma, H.; Mansour, C.; Haddad, M.; Nemer, M.; Stabat, P. Energy consumption and battery sizing for different types of electric bus service. *Energy* **2022**, *239*, 122454. [CrossRef]
16. De Cauwer, C.; Van Mierlo, J.; Coosemans, T. Energy consumption prediction for electric vehicles based on real-world data. *Energies* **2015**, *8*, 8573–8593. [CrossRef]
17. Chen, Y.; Zhang, Y.; Sun, R. Data-driven estimation of energy consumption for electric bus under real-world driving conditions. *Transp. Res. Part D Transp. Environ.* **2021**, *98*, 102969. [CrossRef]
18. Liu, Y.; Liang, H. A data-driven approach for electric bus energy consumption estimation. *IEEE Trans. Intell. Transp. Syst.* **2022**, *23*, 17027–17038. [CrossRef]
19. Nan, S.; Tu, R.; Li, T.; Sun, J.; Chen, H. From driving behavior to energy consumption: A novel method to predict the energy consumption of electric bus. *Energy* **2022**, *261*, 125188. [CrossRef]
20. Dong, C.; Xiong, Z.; Li, N.; Yu, X.; Liang, M.; Zhang, C.; Li, Y.; Wang, H. A real-time prediction framework for energy consumption of electric buses using integrated Machine learning algorithms. *Transp. Res. Part E Logist. Transp. Rev.* **2025**, *194*, 103884. [CrossRef]
21. Ullah, I.; Liu, K.; Yamamoto, T.; Al Mamlook, R.E.; Jamal, A. A comparative performance of machine learning algorithm to predict electric vehicles energy consumption: A path towards sustainability. *Energy Environ.* **2022**, *33*, 1583–1612. [CrossRef]
22. Kivekäs, K.; VepsäläInen, J.; Tammi, K. Stochastic driving cycle synthesis for analyzing the energy consumption of a battery electric bus. *IEEE Access* **2018**, *6*, 55586–55598. [CrossRef]
23. Kivekäs, K.; Lajunen, A.; Vepsäläinen, J.; Tammi, K. City bus powertrain comparison: Driving cycle variation and passenger load sensitivity analysis. *Energies* **2018**, *11*, 1755. [CrossRef]
24. Zhang, Z.; Ye, B.; Wang, S.; Ma, Y. Analysis and estimation of energy consumption of electric buses using real-world data. *Transp. Res. Part D Transp. Environ.* **2024**, *126*, 104017. [CrossRef]
25. Yang, H.; Almutairi, F.; Rakha, H. Eco-driving at signalized intersections: A multiple signal optimization approach. *IEEE Trans. Intell. Transp. Syst.* **2020**, *22*, 2943–2955. [CrossRef]
26. Ozkan, F.; Arslan, M.S.; Mercan, H. Green wave control strategy for optimal energy consumption by model predictive control in electric vehicles. In *Proceedings of the 2024 International Congress on Human-Computer Interaction, Optimization and Robotic Applications (HORA), Istanbul, Turkey, 23–25 May 2024* ; IEEE: New York, NY, USA , 2024; pp. 1–8.
27. Yang, B.; Zhang, Y.; Cai, Z.; Huang, S.T.; Feng, Q. Study on the green wave optimal speed guidance system based on v2x. In *Proceedings of the Society of Automotive Engineers (SAE)-China Congress*; Springer: Berlin/Heidelberg, Germany, 2018; pp. 383–391.
28. Talluri, K.K.; Stang, C.; Weidl, G. Green Wave as an Integral Part for the Optimization of Traffic Efficiency and Safety: A Survey. In Proceedings of the 2025 IEEE Intelligent Vehicles Symposium (IV), Cluj-Napoca, Romania, 22–25 June 2025; pp. 2422–2429. [CrossRef]
29. Bartłomiejczyk, M.; Jagiełło, A.; Wołek, M. The role of bus traffic prioritization in optimizing battery size and reducing the costs of electric buses. *Energies* **2025**, *18*, 6066. [CrossRef]
30. Mahmoud, M.; Garnett, R.; Ferguson, M.; Kanaroglou, P. Electric buses: A review of alternative powertrains. *Renew. Sustain. Energy Rev.* **2016**, *62*, 673–684. [CrossRef]
31. Liu, K.; Gao, H.; Wang, Y.; Feng, T.; Li, C. Robust charging strategies for electric bus fleets under energy consumption uncertainty. *Transp. Res. Part D Transp. Environ.* **2022**, *104*, 103215. [CrossRef]
32. Alamatsaz, K.; Hussain, S.; Lai, C.; Eicker, U. Electric bus scheduling and timetabling, fast charging infrastructure planning, and their impact on the grid: A review. *Energies* **2022**, *15*, 7919. [CrossRef]

33. Zhao, J.; He, J.; Wang, J.; Liu, K. Energy Consumption Prediction for Electric Buses Based on Traction Modeling and LightGBM. *World Electr. Veh. J.* **2025**, *16*, 159. [CrossRef]
34. Göhlich, D.; Fay, T.A.; Jefferies, D.; Lauth, E.; Kunith, A.; Zhang, X. Design of urban electric bus systems. *Des. Sci.* **2018**, *4*, e15. [CrossRef]

Disclaimer/Publisher's Note: The statements, opinions and data contained in all publications are solely those of the individual author(s) and contributor(s) and not of MDPI and/or the editor(s). MDPI and/or the editor(s) disclaim responsibility for any injury to people or property resulting from any ideas, methods, instructions or products referred to in the content.